Electronic Supplementary Information (ESI)

Template-directed synthesis of one-dimensional hexagonal PdTe nanowires for efficient ethanol electrooxidation

Zhenya Hu,[ab] Mengyuan Ma,[ab] Penglei Cui,[a] Hui Liu,[a] Dong Chen,[a] Shaonan Tian,*[a] Lin Xu*[c] and Jun Yang *[ab]

[a] *State Key Laboratory of Mesoscience and Engineering, Institute of Process Engineering, Chinese Academy of Sciences, Beijing 100190, China. Email: sntian@ipe.ac.cn (S.T.); jyang@ipe.ac.cn (J.Y.)*

[b] *Center of Materials Science and Optoelectronics Engineering, University of Chinese Academy of Sciences, Beijing 100049, China*

[c] *School of Chemistry and Materials Science, Jiangsu Key Laboratory of New Power Batteries, Jiangsu Collaborative Innovation Centre of Biomedical Functional Materials, Nanjing Normal University, Nanjing 210023, P. R. China. Email:* xulin001@njnu.edu.cn (L.X.)

Experimental

Chemicals. Sodium tellurite (Na_2TeO_3, 99.5%), poly(vinylpyrrolidone) (PVP, average MW = 58,000), ethylene glycol (EG), sodium tetrachloropalladate (Na_2PdCl_4, 98%), potassium hexachloroplatinate (K_2PtCl_6, 99.9%) were purchased from Sigma–Aldrich. Potassium Hydroxide (KOH, 95%) was bought from Macklin. Aqueous ammonia solution (25–28% w/w%), hydrazine hydrate (85%, w/w%), ethanol (C_2H_5OH, AR), acetone (CH_3COCH_3, AR) were purchased from Sinopharm Chemical Reagent Co. Ltd. (Shanghai, China). Nafion perfluorinated resin solution (5% w/w) was purchased from Dupont. Commercial Pd/C was purchased from Alfa Aesar Chemicals Co., Ltd. The Vulcan XC-72 R carbon black was purchased from Cabot. All the chemicals were used as received. Deionized water (DIW) (18 MΩ cm) was used throughout this study.

Synthesis of Te NWs. The Te NWs were prepared using a reported method developed by the Yu group.[1] For a typical synthesis, 1000 mg of PVP and 88.8 mg of Na_2TeO_3 (0.4 mmol) were dissolved in 35 mL of DIW under vigorous magnetic stirring at room temperature, followed by addition of 1.7 mL of hydrazine hydrate and 3.3 mL of aqueous ammonia solution. The resulting homogeneous solution was then transferred into a Teflon-lined stainless-steel autoclave (100 mL), which was heated to 180℃ for 4 h before cooling down to room temperature. The product was collected by centrifugation and washed with a mixture of ethanol/acetone. Finally, the obtained Te NWs were dispersed in water with a concentration of ca. 0.4 mmol of Te NWs per 20 mL for further use.

Synthesis of PdTe and $PtTe_2$ nanowires. To prepare PdTe NWs, 2 mL of previously

prepared Te NWs was dispersed in 10 mL of ethylene glycol (EG). Afterward, 1 mL of 40 mM Na_2PdCl_4 aqueous solution was added dropwise under vigorous shaking to obtain a homogeneous mixed solution, which was then transferred into a Teflon-lined stainless-steel autoclave (50 mL). The autoclave was heated to 180℃ in 0.5 h and maintained at 180℃ for another 9.5 h before cooling down to room temperature. The PdTe NWs were collected by centrifugation and washed with an ethanol/acetone mixture. The synthesis of $PtTe_2$ NWs was the same as that of PdTe NWs except that 1 mL of 20 mM K_2PtCl_6 aqueous solution were used instead.

Characterization. The transmission electron microscopy (TEM) and high-resolution TEM (HRTEM) images were taken at a JEOL JEM-2010F electron microscope, and an energy dispersive X-Ray spectroscopy (EDX) analyzer attached to the TEM operated in the scanning TEM (STEM) model was used to probe the distributions of relevant elements in the as-prepared samples. Powder XRD patterns of the samples were recorded by a Rigaku SmartLab 9 kW diffractometer using Cu Ka radiation, while X-ray photoelectron spectroscopy (XPS) was conducted on an Axis Supra+ XPS spectrometer for characterizing the chemical states of the relevant elements. The accurate contents of the Pd loading on the carbon substrate were determined by inductively coupled plasma atomic emission spectrometry (ICP-AES, Agilent 5800VDV).

Electrochemical measurements. Before electrochemical measurements, the PdTe NWs were loaded on carbon substrate (denoted as PdTe NWs/C). Electrochemical measurements were conducted on a standard three-electrode cell that was connected to a Bio-logic VMP3 potentiostat. A glassy carbon (GC, diameter: 5 mm, area: 0.196 cm^2) electrode was used as the working electrode. A leak-free Ag/AgCl electrode and a platinum mesh (1 × 1 cm^2) attached to a platinum wire were used as the reference and counter electrode, respectively. All potentials were converted to values with reference to reversible hydrogen electrode (RHE). The catalyst inks were prepared as following: 5 mg of the above-mentioned catalysts was dispersed ultrasonically into a mixed solution containing 0.8 mL of ethanol, 0.15 mL of water and 0.05 mL of Nafion solution. Then, 5 μL of the ink was dropped onto the glassy carbon electrode, followed by drying in a stream of warm air at 70°C. Then, the electrode was connected to a three-electrode test system to measure the electrochemical properties.

For the EOR tests, the cyclic voltammetry (CV) curves of these catalysts were recorded in an N_2-saturated 1 M KOH solution from -1 to 0.2 V (vs. Ag/AgCl electrode) at a scan rate of 200 mV s^{-1}, 100 mV s^{-1} and 50 mV s^{-1} for 20 cycles, respectively, to clean and stabilize the catalyst surfaces. Subsequently, the electrolyte was replaced by 1 M KOH solution containing 1 M ethanol. The catalytic performance for the ethanol oxidation was measured at room temperature by CV. For these measurements, the potential window of -1–0.2 V versus Ag/AgCl was scanned at a rate of 50 mV s^{-1}. For the chronoamperometry (CA) tests, the curves were recorded at 0.63 V in a solution containing 1 M KOH and 1 M ethanol. For the ten consecutive chronoamperometry tests (36000 s for total and 3600 s for each cycle), the curves were recorded after the electrolyte was substitute for a fresh solution containing 1 M KOH and 1 M ethanol each time. Before the chronoamperometry tests,

the CV were conducted at a scan rate of 50 mV s^{-1} for 10 cycles to remove the accumulated toxic intermediates on the active sites. For the CO stripping, the catalysts undergo electrochemical pre-treatment by potential cycling in an N_2-saturated 1 M KOH electrolyte. Next, the working electrode was maintained in a CO-saturated solution for 20 min to complete the adsorption of CO onto the catalyst. The electrochemical CO stripping voltammograms were obtained in 1 M KOH at a scan rate of 50 mV s^{-1}.

The electrochemically active surface areas (ECSAs) of these Pd-based nanoparticles were determined by stripping a Cu monolayer that was deposited on the electrode through Cu underpotentially deposition (Cuupd) method. For the Cu stripping experiments, the CVs of different catalysts were first obtained in N_2-saturated 0.05 M H_2SO_4 from -0.2 V to 1 V (vs. Ag/AgCl) at 20 mV s^{-1}. Subsequently, the potential was first held at 0.3 V (vs. RHE) for 100 s to form a Cuupd monolayer, and then CVs were obtained in a N_2-saturated solution containing 2 mM $CuSO_4$ and 0.05 M H_2SO_4 solution. the ECSAs were calculated using the following formula: ECSAs = Q/470G, where Q is the charge of the CV curves in $CuSO_4$ and H_2SO_4 solution by subtracting the background CVs that were collected in H_2SO_4 solution, which is calculated by dividing the scan rate (20 mV s^{-1}), G represents the mass loading of Pd (μg) on the electrode determined by ICP-AES, and 470 is the theoretical charge density (μC cm^{-2}).

Table S1. Electrochemically active surface areas (ECSAs) and Pd contents of the PdTe NWs/C and commercial Pd/C catalyst as well as their EOR performances in the alkaline medium.

Catalyst	ECSA ($m^2\ g^{-1}$)	Pd content (wt%)	Mass activity ($A\ mg_{Pd}^{-1}$)	Specific activity ($mA\ cm^{-2}$)
PdTe NWs/C	46.9	14.5	4.4	9.4
Pd/C	38.3	20.0	1.3	3.4

Table S2. EOR performances of the hexagonal PdTe nanowires and various Pd-based electrocatalysts reported recently.

Catalyst	Electrolyte	Noble metal mass on electrode (ug/cm^2)	Mass Activity (A mg_{Pd}^{-1})	Rate (mV s^{-1})	Refs.
PdTe NWs/C	1.0 M KOH + 1.0 M ethanol	~18.5	4.4	50	This work
$Pd_{14.9}Bi$	1.0 M KOH + 1.0 M ethanol	NA	5.74	50	2
Pd-PdSe nanosheets	1.0 M KOH + 1.0 M ethanol	NA	5.9	50	3
Pd-Ni-P	1.0 M NaOH + 1.0 M ethanol	20	4.95	100	4
PdRhTe	1.0 M KOH + 1.0 M ethanol	NA	2.039	50	5
HD-PdZn NCs	1.0 M KOH + 1.0 M ethanol	NA	3.45	50	6
PdAg	1.0 M KOH + 1.0 M ethanol	NA	1.95	50	7
PdSb	0.5 M NaOH + 0.5 M ethanol	25.5	4.5	20	8
$PdCu_2$	1.0 M KOH + 1.0 M ethanol	NA	1.63	50	9
PdP nanosheets	1.0 M KOH + 1.0 M ethanol	~37	3.2	50	10
$Pd/Ni(OH)_2/rGO$	1.0 M KOH + 1.0 M ethanol	NA	1.546	50	11
PdZn	1 M NaOH + 1 M ethanol	~14.3	2.73	50	12
Au@PdAu	1.0 M KOH + 1.0 M ethanol	~2.55 (Pd)	47.8	50	13
PdSn-NbN/C	1.0 M KOH + 1.0 M ethanol	~5.84	15.1	50	14
NIR-Spilky Au@AuPd	0.5 M KOH + 1.0 M ethanol	NA	33.2	20	15

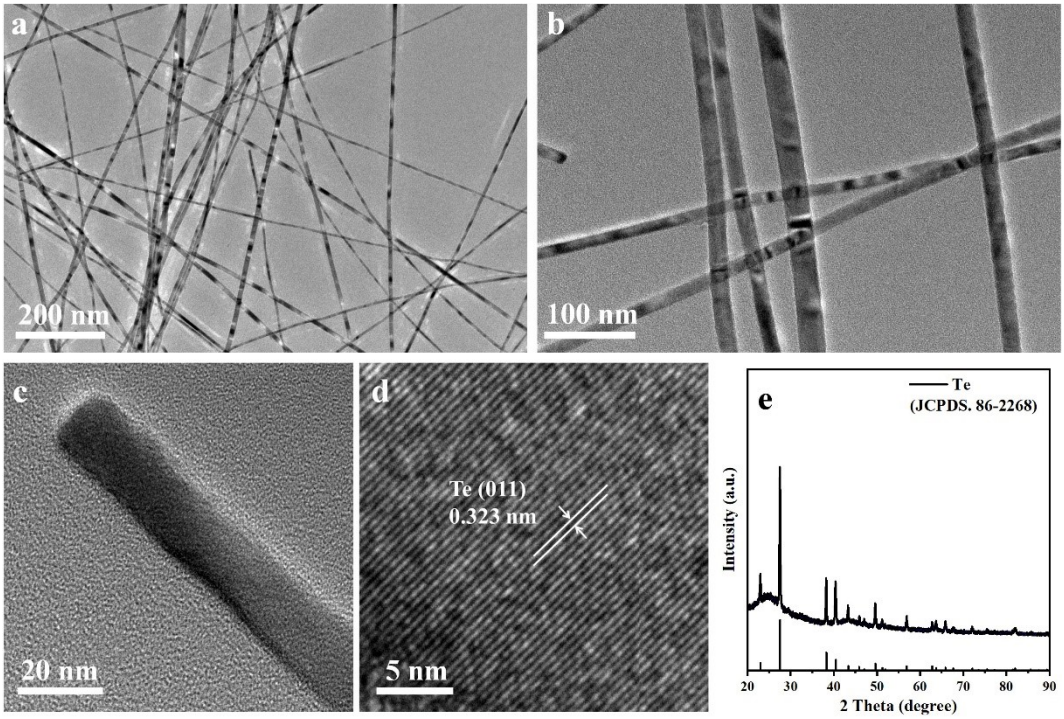

Fig. S1 (a–c) TEM images with different magnifications, (d) HRTEM image, and (e) XRD pattern of the Te nanowires served as template.

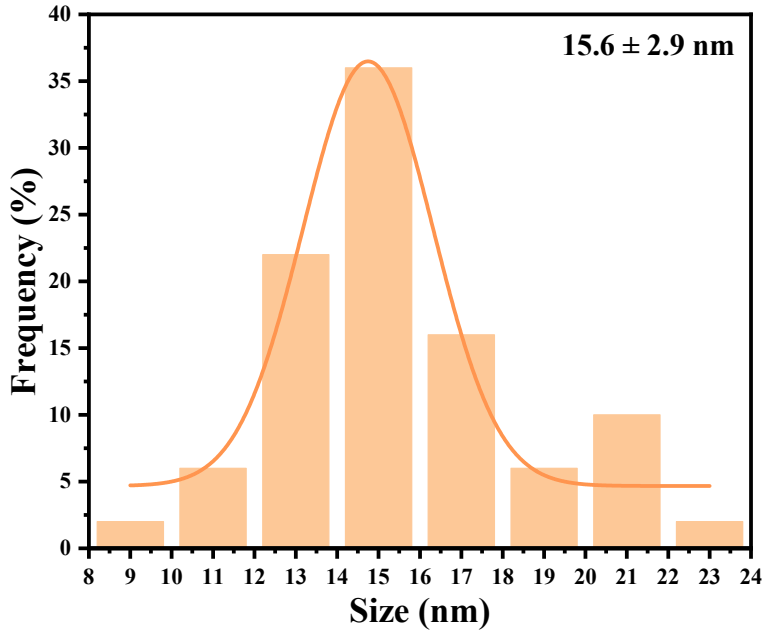

Fig. S2 Histogram showing the particle diameter distribution of the Te NWs prepared as template by hydrothermal synthesis.

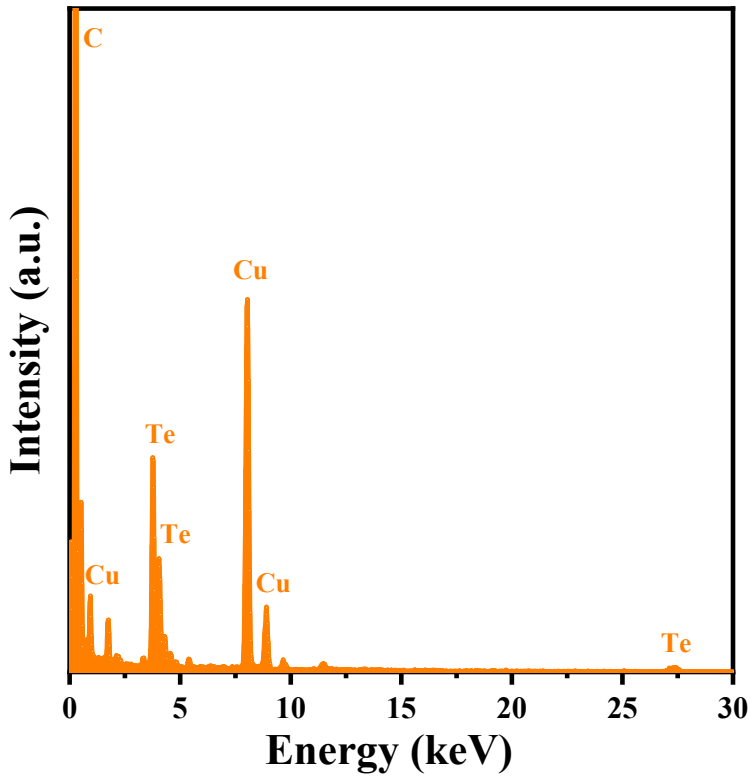

Fig. S3 Energy-dispersive X-ray (EDX) spectrum of the Te NWs prepared as template by hydrothermal synthesis.

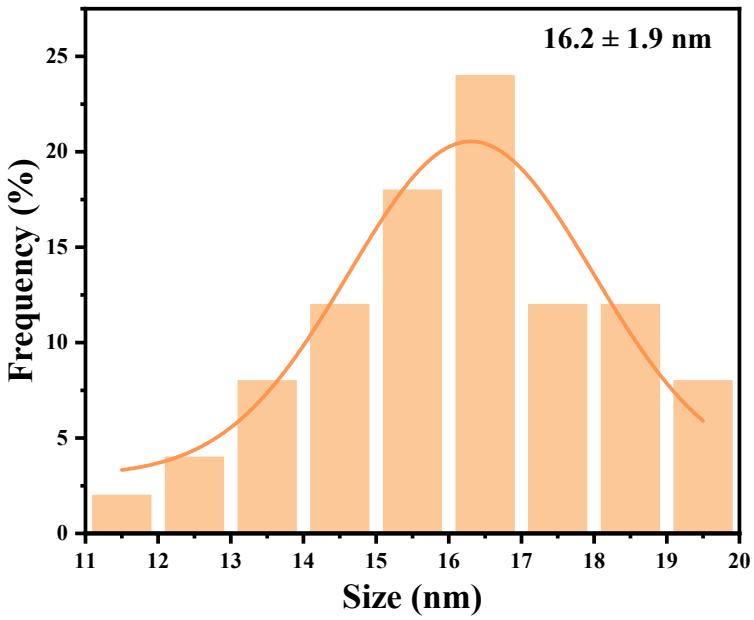

Fig. S4 Histogram showing the particle diameter distribution of the PdTe NWs prepared by using Te NWs as template through hydrothermal synthesis

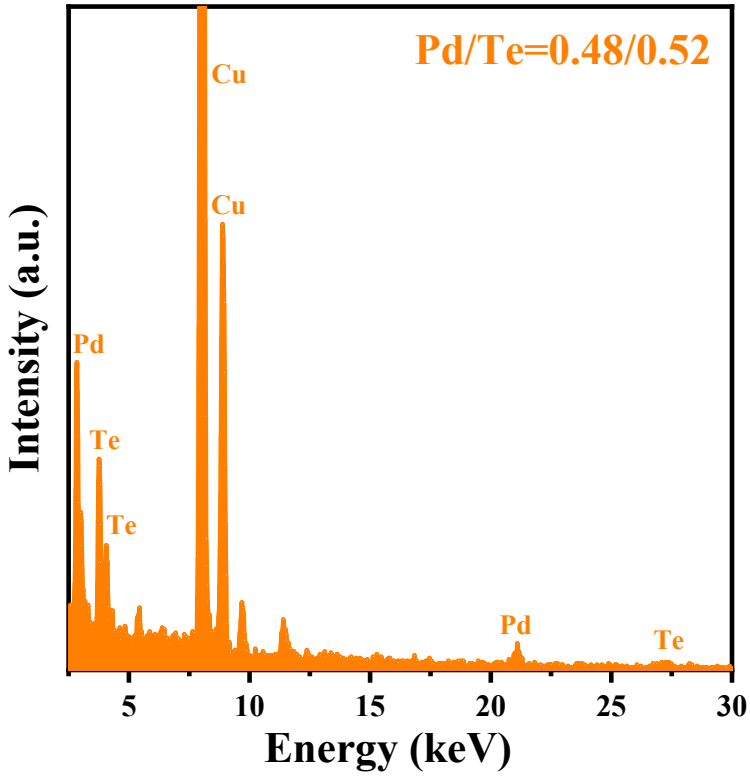

Fig. S5 Energy-dispersive X-ray (EDX) spectrum of the PdTe NWs prepared using Te NWs as template through hydrothermal synthesis.

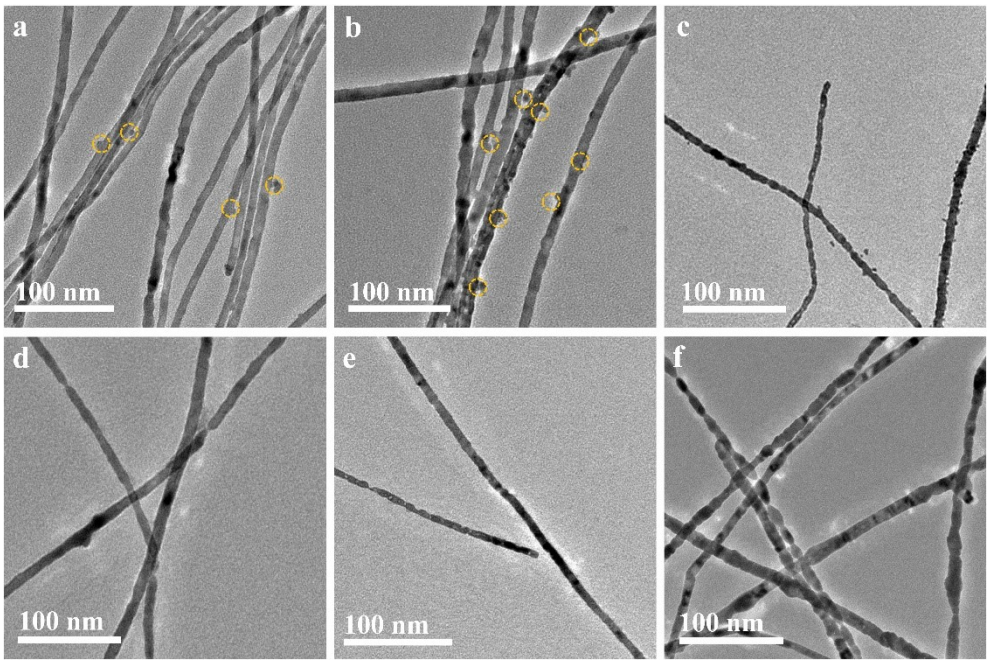

Fig. S6 TEM images of a series of samples obtained after reaction for (a) 15 min, (b) 30 min, (c) 1 h, (d) 2 h, (e) 5 h, and (f) 10 h, respectively, in ethylene glycol at 180°C.

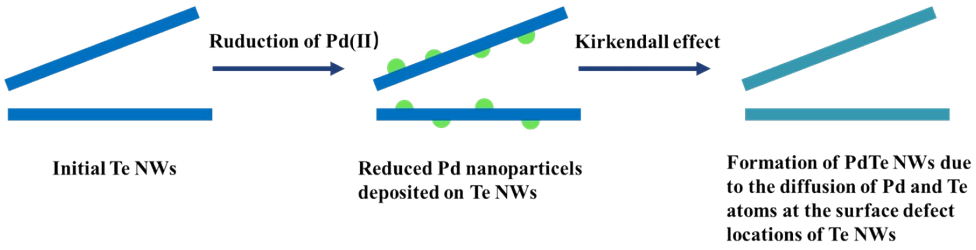

Fig. S7 Schematic diagram showing the synthetic mechanism for hexagonal PdTe NWs using Te NWs as template.

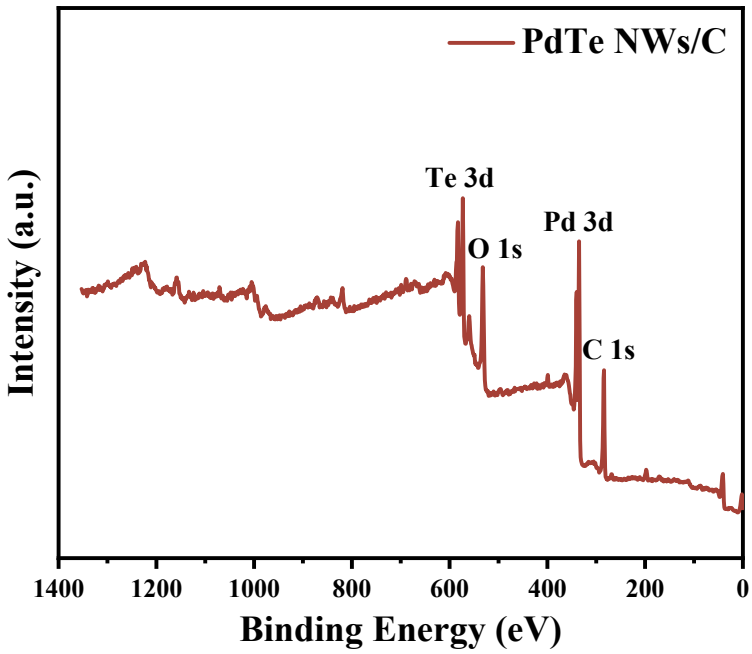

Fig. S8 Full XPS spectrum of the PdTe NWs prepared using Te NWs as template through hydrothermal synthesis.

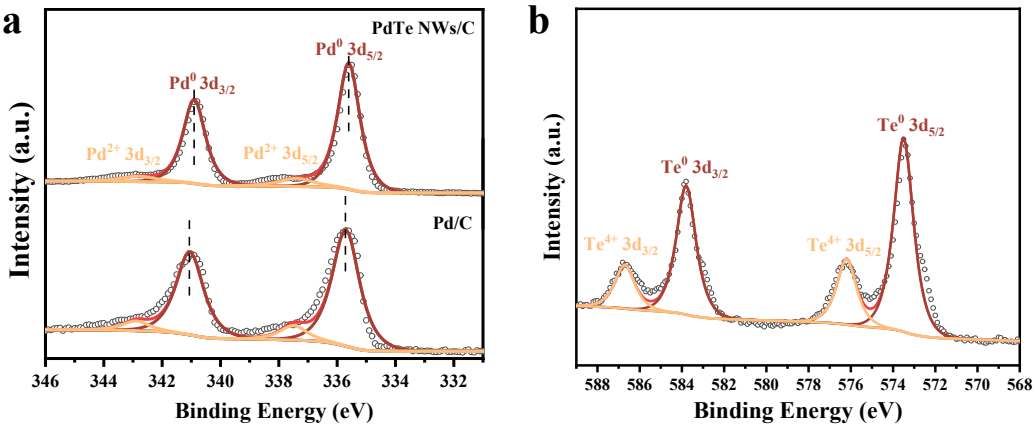

Fig. S9 (a) Pd 3d XPS spectra of the hexagonal PdTe NWs and commercial Pd/C; (b) Te 3d XPS spectrum of the PdTe NWs.

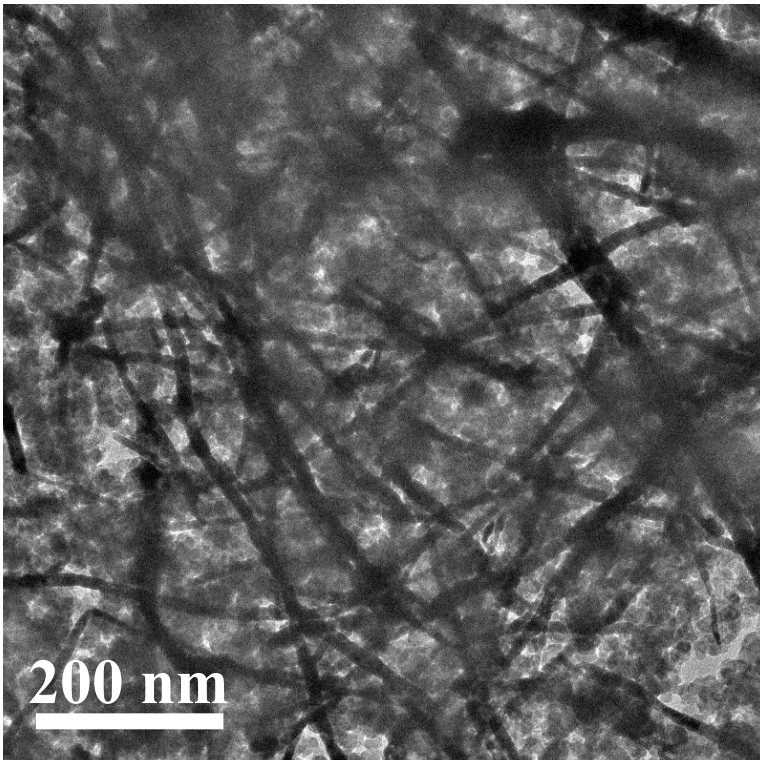

Fig. S10 TEM image of the PdTe NWs supported on the commercial Vulcan XC-72 carbon substrate.

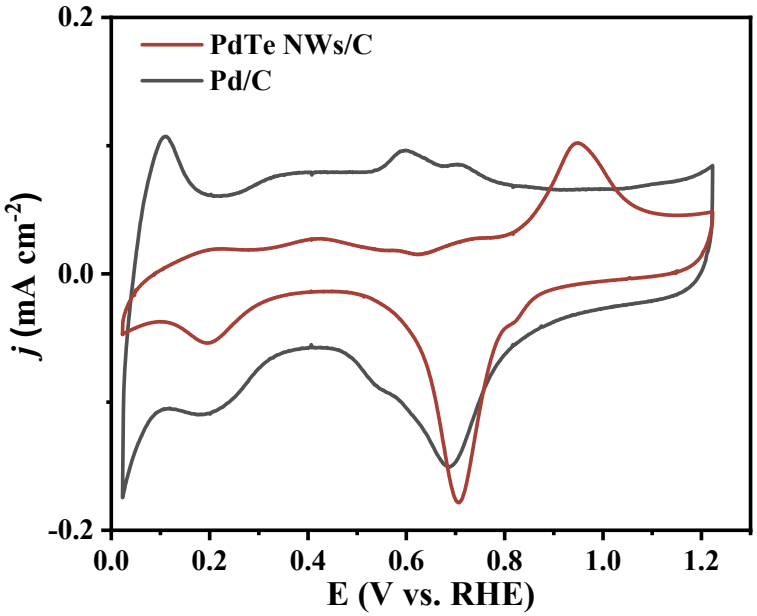

Fig. S11 The cyclic voltammetry (CV) curves of the PdTe NWs/C and commercial Pd/C in 1 M KOH solution.

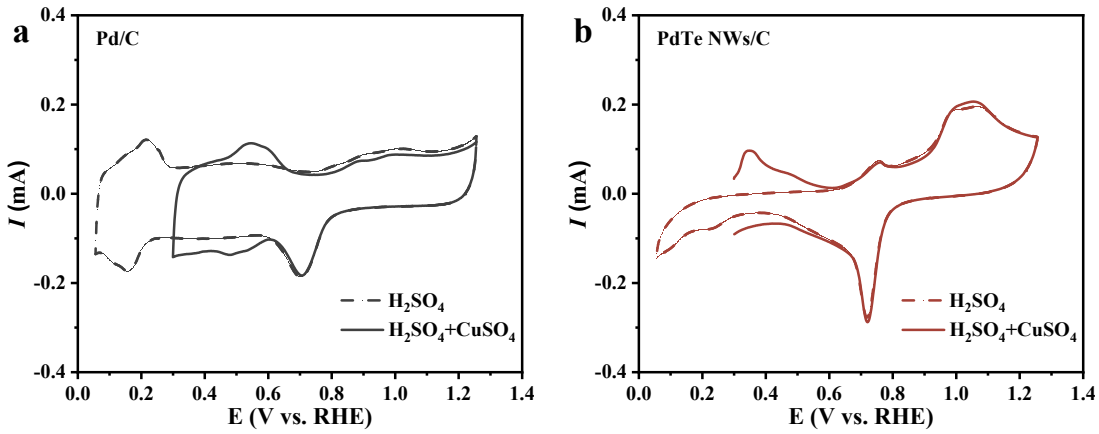

Fig. S12 CV curves and Cu stripping voltammograms of commercial Pd/C and PdTe NWs/C. The CV curves were conducted in 0.05 M H_2SO_4, whereas the Cu stripping voltammograms were conducted in 0.05 M H_2SO_4 + 2 mM $CuSO_4$. Scan rate, 20 mV s^{-1}.

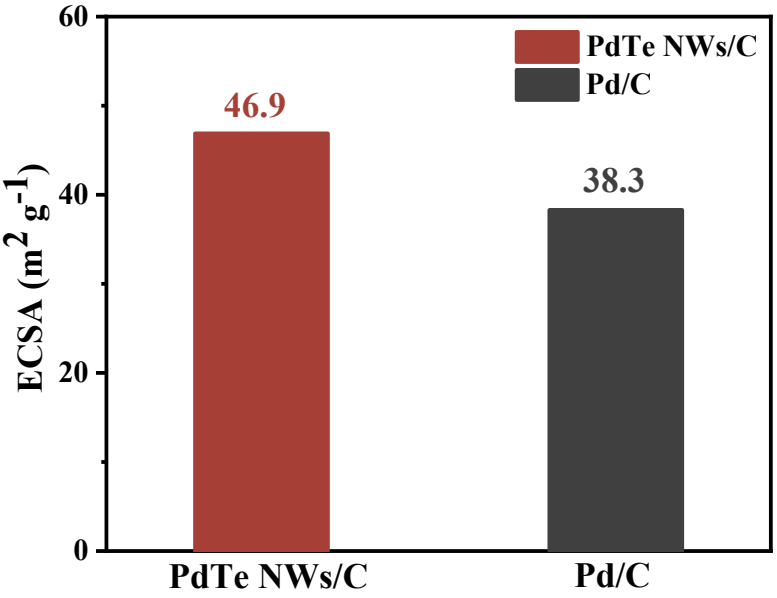

Fig. S13 The electrochemical active surface areas (ECSAs) of the PdTe NWs/C and commercial Pd/C obtained by Cuupd method.

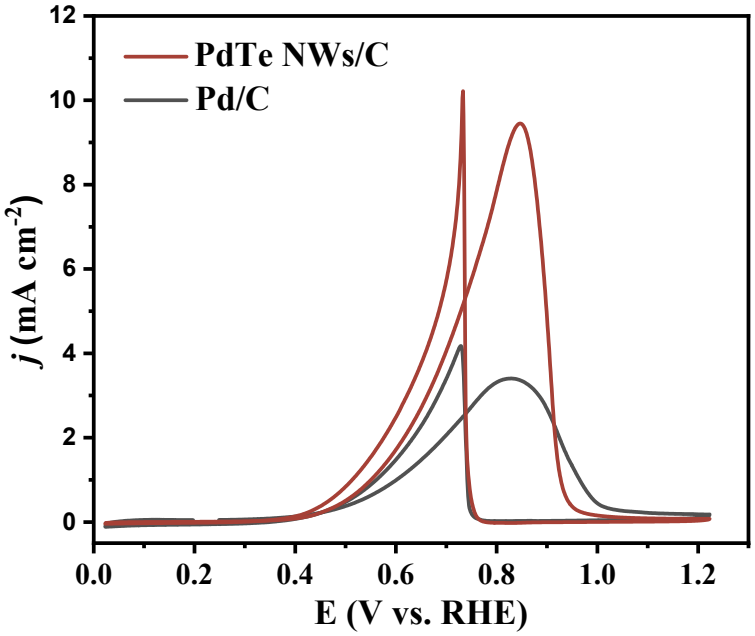

Fig. S14 Specific activities of the PdTe NWs/C and commercial Pd/C for EOR in 1 M KOH + 1 M ethanol solution.

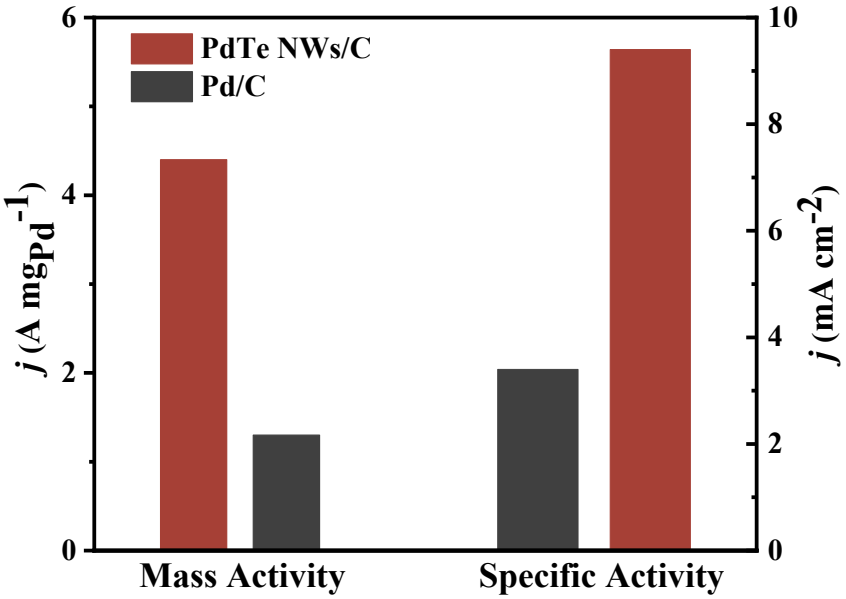

Fig. S15 Column chart showing the comparison of specific and mass activities of the PdTe NWs/C and commercial Pd/C catalyst.

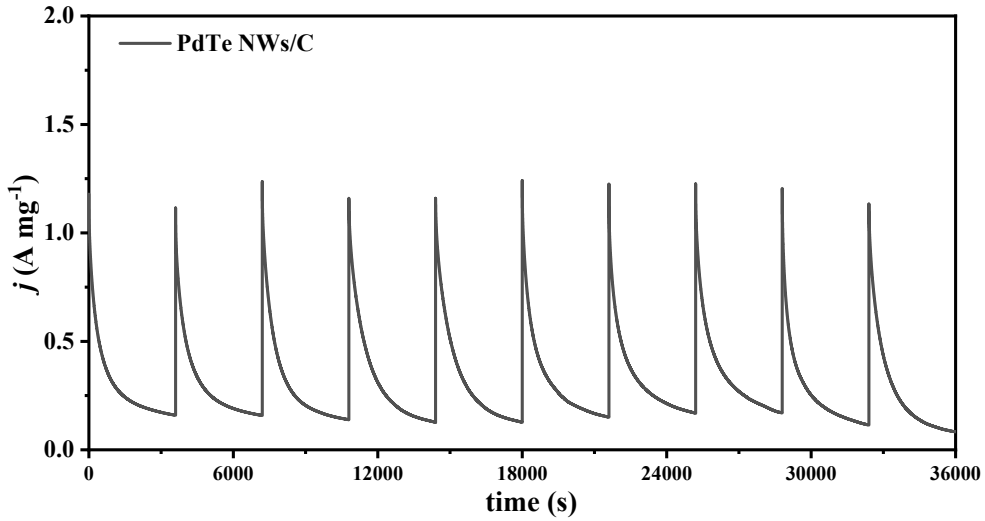

Fig. S16 Ten consecutive cycles of the PdTe NWs/C in a fresh 1 M KOH containing 1 M ethanol (36000 s for total and 3600 s for each cycle).

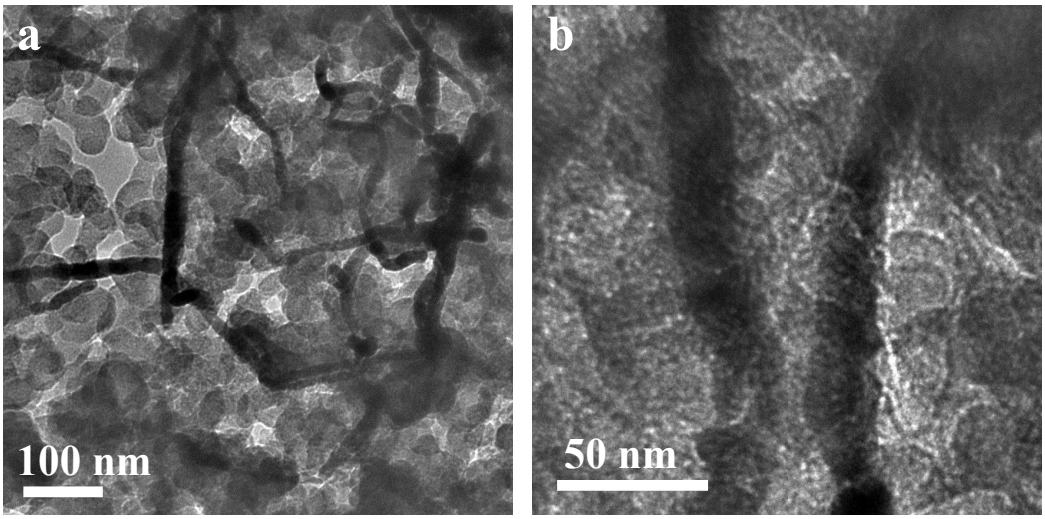

Fig. S17 TEM images of the PdTe NWs/C after electrochemical stability test in 1 M KOH + 1 M ethanol electrolyte.

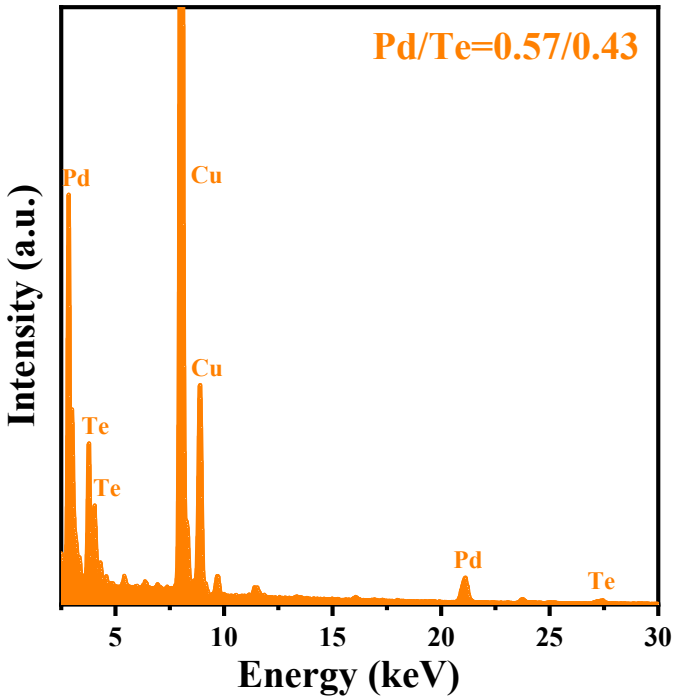

Fig. S18 EDX spectrum showing thePd/Te ratio in the PdTe NWs/C after stability test in 1 M KOH + 1 M ethanol electrolyte.

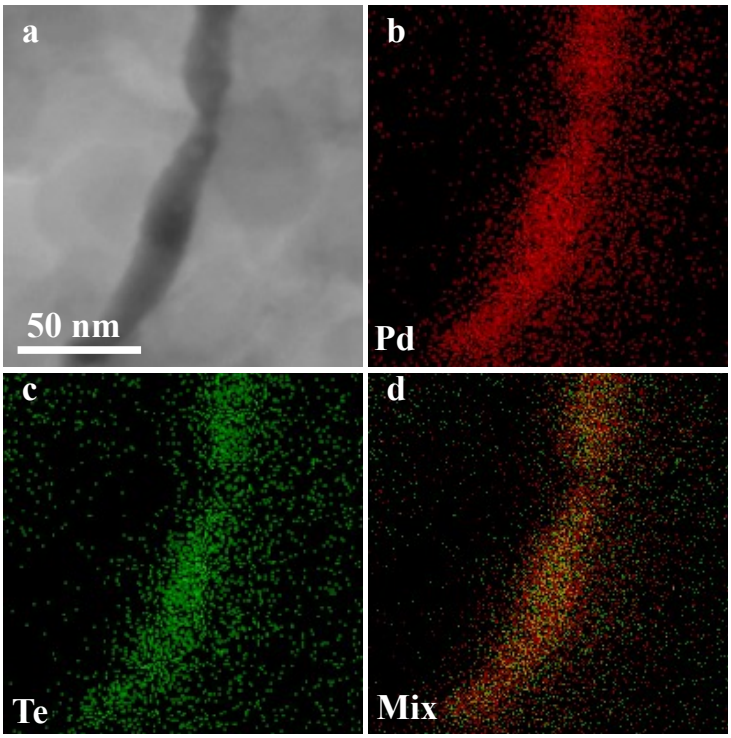

Fig. S19 (a) STEM image and (b–c) corresponding EDX-based element maps of the PdTe NWs/C after stability test in 1 M KOH + 1 M ethanol electrolyte.

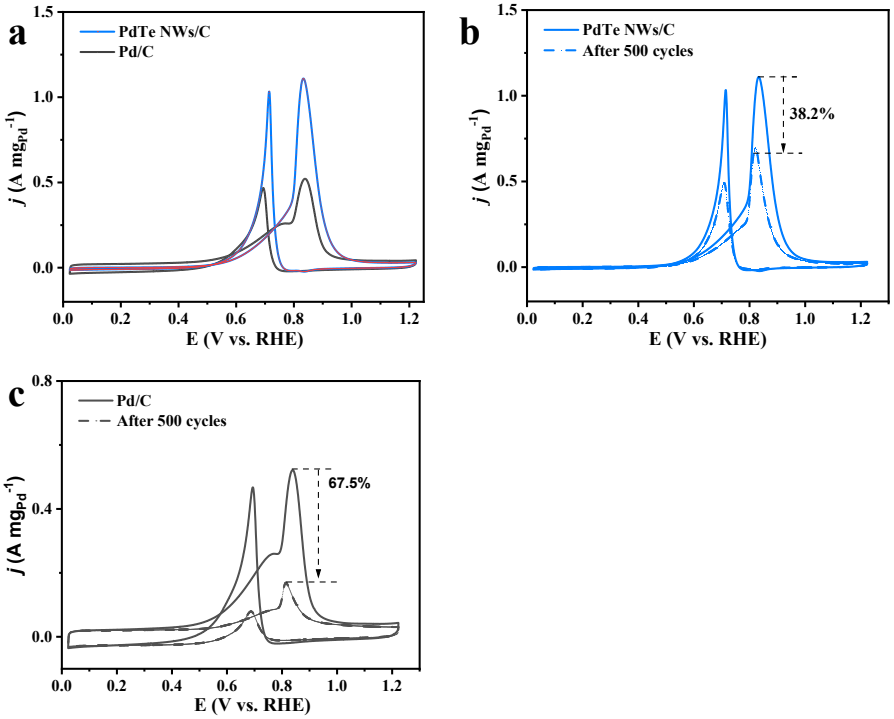

Fig. S20 (a) CV curves of the PdTe NWs/C and commercial Pd/C in 1 M KOH + 1 M methanol solution; CVs of (b) the PdTe NWs/C and (c) Pd/C catalyst before and after 500 CV cycles.

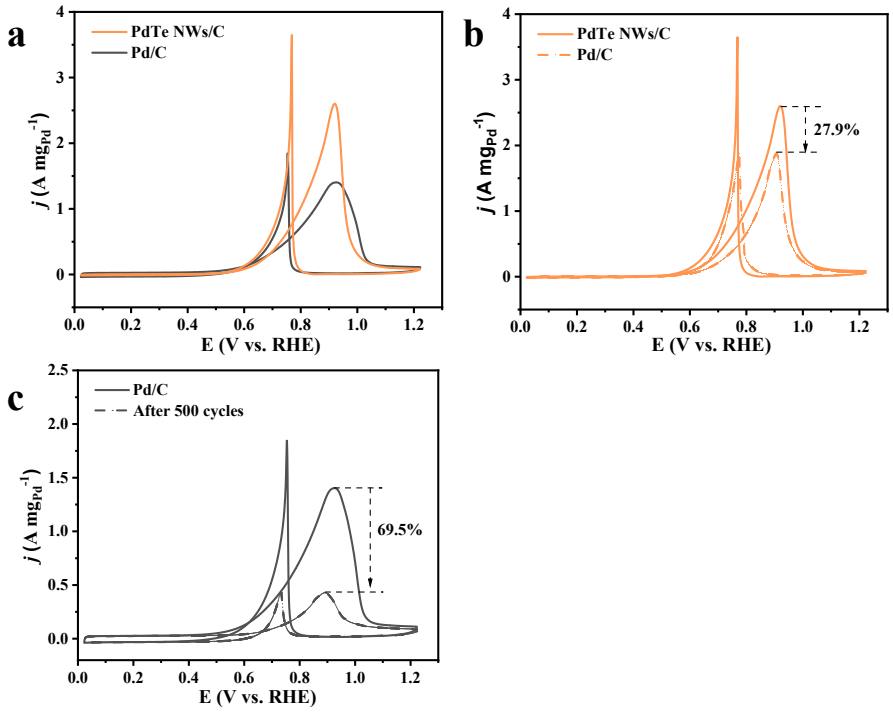

Fig. S21 (a) CV curves of the PdTe NWs/C and commercial Pd/C in 1 M KOH + 1 M ethylene glycol solution; CVs of (b) the PdTe NWs/C and (c) Pd/C catalyst before and after 500 CV cycles.

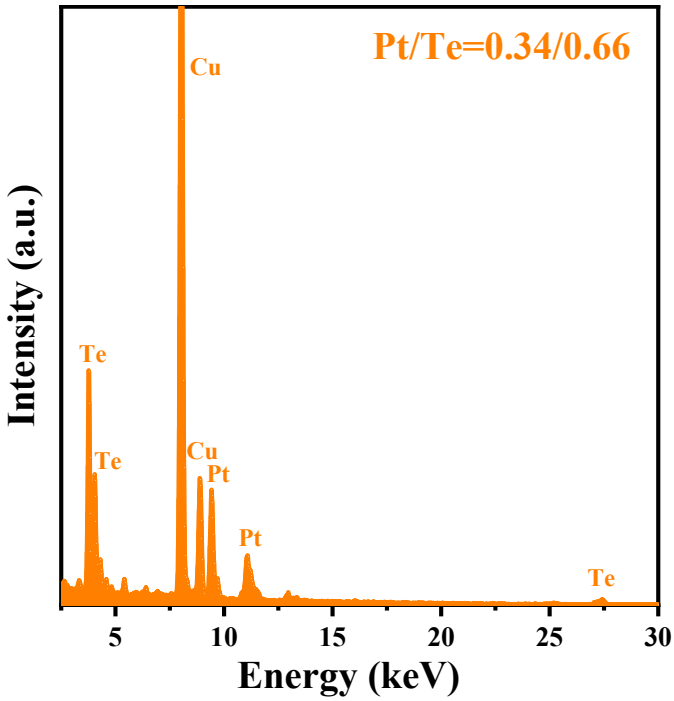

Fig. S22 EDX spectrum of the as-synthesized $PtTe_2$ NWs using Te NWs as template through a hydrothermal process.

Supplementary references

1 H.W. Liang, S. Liu, J.-Y. Gong, S.-B. Wang, L. Wang and S.-H. Yu, *Adv. Mater.*, 2009, **21**, 1850.

2 H. Wang, J. Jiao, L. Zheng, Q. Fang, Y. Qin, X. Luo, X. Wei, L. Hu, W. Gu, J. Wen and C. Zhu, *Adv. Funct. Mater.*, 2021, **31**, 2103465.

3 Y. Qin, W. Zhang, F. Wang, J. Li, J. Ye, X. Sheng, C. Li, X. Liang, P. Liu, X. Wang, X. Zheng, Y. Ren, C. Xu and Z. Zhang, *Angew. Chem. Int. Ed.*, 2022, **61**, e202200899.

4 L. Chen, L. Lu, H. Zhu, Y. Chen, Y. Huang, Y. Li and L. Wang, *Nat. Commun.*, 2017, **8**, 14136.

5 J. Jin, H. Xu, C. Chen, H. Shang, Y. Wang and Y. Du, *Inorg. Chem.*, 2019, **58**, 12377.

6 S. Huang, S. Lu, H. Hu, F. Xu, H. Li, F. Duan, H. Zhu, H. Gu and M. Du, *Chem. Eng. J.*, 2021, **420**, 130503.

7 L. Yang, F. Gao, L. Xu, B. Fu, Y. Zheng and P. Guo, *ACS Appl. Energy Mater.*, 2022, 5, 11624.

8 Y. Zhang, X. Liu, T. Liu, X. Ma, Y. Feng, B. Xu, W. Cai, Y. Li, D. Su, Q. Shao and X. Huang, *Adv. Mater.*, 2022, **34**, 2202333.

9 J. Xue, G. Han, W. Ye, Y. Sang, H. Li, P. Guo and X. S. Zhao, *ACS Appl. Mater. Interfaces*, 2016, **8**, 34497.

10 H. Lv, Y. Teng, Y. Wang, D. Xu and B. Liu, *Chem. Commun.*, 2020, **56**, 15667.

11 W. Huang, X.-Y. Ma, H. Wang, R. Feng, J. Zhou, P. N. Duchesne, P. Zhang, F. Chen, N. Han, F. Zhao, J. Zhou, W.-B. Cai and Y. Li, *Adv. Mater.*, 2017, **29**, 1703057.

12 Q. Yun, Q. Lu, C. Li, B. Chen, Q. Zhang, Q. He, Z. Hu, Z. Zhang, Y. Ge, N. Yang, J. Ge, Y.-B. He, L. Gu and H. Zhang, *ACS Nano*, 2019, **13**, 14329.

13 X. Wang, H. Yang, M. Liu, Z. Liu, K. Liu, Z. Mu, Y. Zhang, T. Cheng and C. Gao, ACS Nano, 2024, **18**, 18701.

14 N. Ye, W. Sheng, R. Zhang, B. Yan, Z. Jiang and T. Fang, Small. 2024, **20**, 2304990.

15 M. Zhang, X. Zhang, M. Lv, X. Yue, Z. Zheng and H. Xia, Small, 2023, **19**, 2205781.